Journal of Inflammation Research

Dovepress
Taylor & Francis Group

Open Access Full Text Article

ORIGINAL RESEARCH

Dihydromyricetin Improves Ulcerative Colitis by Suppressing NLRP3 Inflammasome Activation Caused by Dysbiosis of Gut Microbiota

Jun Chen[1,2,*], Shengchen Ding[1,2,*], Huabing Yang[1,2], Yi Dai[3], Zhigang Zhang[1,2], Tianxiang Zhu[1,2], Lu Cao[1,2], Baifei Hu[1,2], Hongtao Liu[1,2,4]

[1]College of Basic Medical Sciences, Hubei University of Chinese Medicine, Wuhan, 430065, People's Republic of China; [2]Hubei Shizhen Laboratory, Wuhan, 430061, People's Republic of China; [3]Wuhan Hospital of Traditional Chinese Medicine, Wuhan, 430022, People's Republic of China; [4]Key Laboratory of Chinese Medicinal Resource and Chinese Herbal Compound of the Ministry of Education, Wuhan, 430065, People's Republic of China

*These authors contributed equally to this work

Correspondence: Baifei Hu; Hongtao Liu, Email baifeihu3452@hbucm.edu.cn; hongtaoliu@hbucm.edu.cn

Purpose: Dihydromyricetin (DMY) is known for its wide range of pharmacological effects and has been approved as a dietary supplement. This study aimed to investigate the therapeutic effects of DMY on dextran sulfate sodium (DSS)-induced disruption of intestinal homeostasis in mice and to explore the underlying molecular mechanisms.

Methods: To establish a model of colitis, mice were treated with a 3% DSS solution, followed by gavage administration of DMY for therapeutic intervention. Techniques such as histomorphology, RT-qPCR, 16S rRNA sequencing, and Western blot analysis were used.

Results: DMY alleviated several physiological symptoms in colitis mice, including a reduction in the disease activity index (DAI) and spleen index, as well as decreases in the numbers of white blood cells, lymphocytes, and monocytes. Additionally, DMY helped repair the intestinal mucosal barrier function, reshaped the composition of gut microbiota, and regulated intestinal immune responses. These effects collectively contributed to the partial restoration of intestinal homeostasis in colitis mice. Furthermore, experiments with NLRP3$^{-/-}$ mice and pseudo-germ-free mice confirmed that DMY exerts its anti-colitis effects through the gut microbiota-NLRP3 inflammasome axis.

Conclusion: DMY helps regulate intestinal homeostasis in colitis mice by suppressing the NLRP3 inflammasome via the gut microbiota. Our study provides new evidence supporting DMY as a potential therapeutic agent for colitis.

Keywords: dihydromyricetin, ulcerative colitis, NLRP3 inflammasome, gut microbiota, intestinal homeostasis

Introduction

Colitis is a chronic, recurrent inflammatory bowel disease.[1] Its clinical manifestations typically include symptoms such as abdominal pain, diarrhea, superficial mucosal ulcers, and bloody stools, as well as extraintestinal symptoms like weight loss and fever.[2,3] Colitis can also lead to long-term complications, such as anemia. It was estimated that the global incidence of colitis reached 5 million cases, with its prevalence showing a consistent upward trend worldwide.[4] This trend highlights colitis as an increasingly significant global health concern.[5] The primary treatment options for colitis currently include aminosalicylates, corticosteroids, and immunosuppressants. However, these treatments often have considerable drawbacks, including notable side effects, high costs, and a tendency for recurrence.[6] As a result, there is a pressing need for the development of new biologics and small-molecule drugs, as well as safer and more effective treatment options for colitis.

The pathogenesis of colitis is complex, with the imbalance of intestinal homeostasis recognized as a key factor contributing to its chronic nature and frequent relapses.[7] Intestinal homeostasis is maintained through the interplay between the intestinal barrier, gut microbiota, and the immune system.[8] The intestinal barrier serves to prevent harmful

Received: 7 June 2025
Accepted: 21 November 2025
Published: 13 December 2025

Graphical Abstract

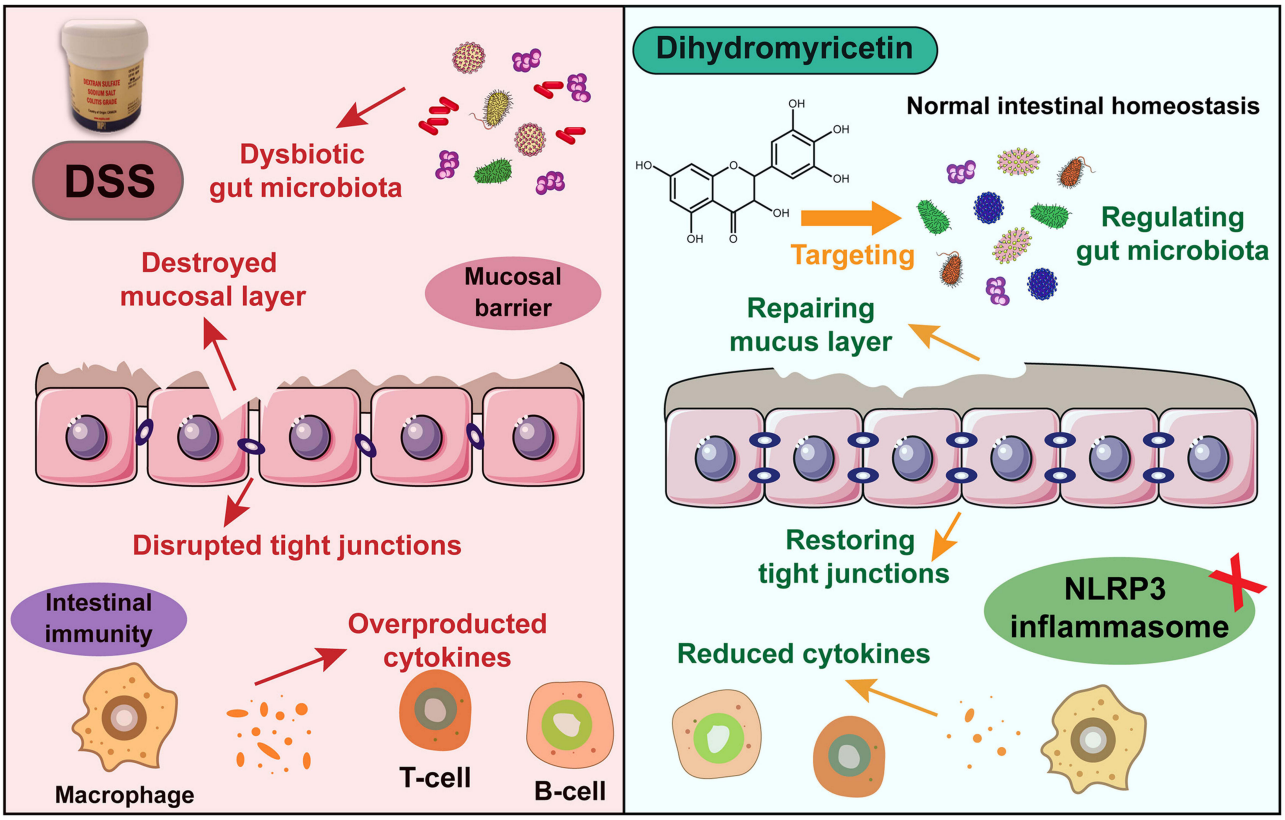

substances and pathogens from entering the body's internal environment.[9,10] Various intestinal diseases, including colitis, compromise this mucosal barrier, leading to structural changes that represent an initial disruption of homeostasis.[11] As the intestinal barrier becomes damaged, symbiotic microorganisms in the intestinal lumen can translocate into the lamina propria of the intestinal mucosa, triggering an abnormal immune response.[12] This response is characterized by a significant increase in inflammatory mediators in the gut. These mediators activate immune cells, resulting in a substantial release of pro-inflammatory cytokines and chemokines, which further intensifies the inflammatory response and exacerbates the disruption of intestinal homeostasis, ultimately leading to gut dysfunction.[13,14] Key molecular pathways involved in this inflammatory cascade include the NOD-like receptor pyrin domain-containing 3 (NLRP3) inflammasome pathway, the nuclear factor kappa B (NF-κB) signaling pathway, and the Toll-like receptor (TLR) signaling pathway. All of these pathways play crucial roles in orchestrating the inflammatory response.[15] Emerging evidence indicates that gut microbiota-derived metabolites, particularly short-chain fatty acids such as butyrate, play a critical role in modulating NLRP3 activation through mechanisms including GAPDH lactylation and butyrylation. These findings further underscore the significance of the microbiota–immune axis in colitis pathogenesis and highlight gut dysbiosis as a potential therapeutic target.[16]

Dihydromyricetin (DMY) is a naturally occurring dihydroflavonol compound that belongs to the flavonoid class of chemical derivatives.[17] DMY is primarily found in vine tea (also known as Mei tea), the concentration of which can reach as high as 30–40% (w/w).[18] It is widely recognized for its diverse pharmacological properties and has been approved as a nutritional supplement.[19,20] Recent pharmacological studies demonstrate that DMY exhibits significant activities, including anti-inflammatory, antioxidant, antitumor, and liver protective effects.[21,22] Notably, its anti-inflammatory properties are particularly impressive. For instance, DMY can effectively reduce methotrexate-induced

hepatotoxicity by inhibiting the TLR4/NF-κB and NLRP3 inflammasome/caspase-1 signaling pathways. Additionally, it can alleviate rheumatoid arthritis by suppressing the overexpression of pro-inflammatory cytokines.[23,24] As a result, DMY has been widely utilized as an effective anti-inflammatory agent. In a previous report, it was noted that DMY helps alleviate colitis induced by dextran sulfate sodium (DSS).[25] However, the mechanisms through which DMY promotes intestinal homeostasis are still not fully understood.

This study aimed to investigate how DMY influences intestinal homeostasis in mice with colitis, specifically by focusing on intestinal barrier function, gut microbiota, and immune responses. Additionally, we explored the crucial role of the NLRP3 inflammasome in the protective effects of DMY against colitis.

Materials and Methods

Reagents

Dextran sulfate sodium (DSS), with a molecular weight of 36–50 kDa, was obtained from MP Biochemicals (Santa Ana, CA, USA). Dihydromyricetin (DMY), which has a purity of 98%, was sourced from Yuanye BioTechnology Co., Ltd. (Shanghai, China). The antibiotics used in the study, including ampicillin, neomycin sulfate, vancomycin, and metronidazole, were supplied by Aladdin Reagent, Inc. (Shanghai, China). All other chemicals utilized in the research were of analytical grade or the highest purity available.

The primary antibodies for β-Actin, iNOS, p-ERK, and ERK1/2 were obtained from Santa Cruz Biotechnology (Santa Cruz, CA, USA). Antibodies targeting COX-2, NLRP3, Cleaved IL-1β, p-JNK, and JNK were sourced from Cell Signaling Technology (Danvers, MA, USA). Antibodies against ASC and MPO were provided by ELK Biotechnology (Denver, CO, USA), while antibodies for F4/80 and Caspase-1 were supplied by ABclonal Technology (Wuhan, China).

Animal Experiments

Six-week-old male C57BL/6J mice, weighing 22 ± 2 g, were obtained from the Hubei Provincial Center for Disease Control and Prevention in Wuhan, China. All mice were housed under controlled environmental conditions, maintaining a temperature of 23 ± 2 °C and a 12-hour light/dark cycle. They had ad libitum access to sterile water and a standard chow diet. After a one-week acclimatization period, the mice were randomly assigned to five groups (n = 8): Control group (Ctrl), DSS-treated group (DSS), DSS + low-dose DMY group (DSS + DMY-L), DSS + medium-dose DMY group (DSS + DMY-M), and DSS + high-dose DMY group (DSS + DMY-H). The Ctrl group received distilled water throughout the experimental period, while the other groups were administered 3% DSS (w/v) in their drinking water for 7 days to induce colitis. During this same period, the DSS + DMY-L, DSS + DMY-M, and DSS + DMY-H groups were given DMY intragastrically at doses of 25 mg/kg/day, 50 mg/kg/day, and 75 mg/kg/day, respectively, dissolved in 2% cyclodextrin. The Ctrl and DSS groups received an equivalent volume of the vehicle solution (2% cyclodextrin).

Male C57BL/6J wild-type (WT) mice and *Nlrp3* knockout (KO) mice were purchased from Saiye Biotechnology Co., Ltd. (Suzhou, China). After a one-week acclimatization period, the mice were randomly assigned to four groups (n = 8): WT-Control (WT-Ctrl), WT-Dextran Sulfate Sodium (WT-DSS), *Nlrp3* KO-DSS, and *Nlrp3* KO-DSS combined with DMY (*Nlrp3* KO-DSS + DMY). The WT-Ctrl group received distilled water, while the other groups were administered a 3% solution of DSS in their drinking water for a duration of seven days. Additionally, the *Nlrp3* KO-DSS + DMY group was given DMY at a dosage of 75 mg/kg/day, dissolved in 2% cyclodextrin, via gavage for the same seven days.

To create the pseudo-germ-free mouse model, male C57BL/6J mice were randomly divided into four groups (n=8): Ctrl, DSS, DSS + Abx, and DSS + Abx + DMY. Mice in the DSS + Abx and DSS + Abx + DMY groups received an antibiotic mixture (Abx) containing 1 g/L ampicillin, 1 g/L neomycin sulfate, 0.5 g/L vancomycin, and 0.5 g/L metronidazole, all dissolved in sterile water for free drinking. After eight weeks of Abx treatment, fecal bacterial genomic DNA was extracted and quantified to confirm the depletion of the gut microbiota (Supplementary Methods 3, Supplementary Figure S2, and Supplementary Table 4). During the final week, 3% DSS was administered to induce colitis, and mice in the DSS + Abx + DMY group additionally received DMY (75 mg/kg/day) by oral gavage. Administration routes and dosages were consistent with those described previously.

During the animal experiments, we monitored body weight, diet, and water intake daily for each group of mice. All mice were deeply anesthetized and euthanized using isoflurane gas inhalation after the treatment. We collected and photographed colon tissues, and measured the colon length. Additionally, spleens were weighed to assess changes in organ indices. Samples were stored at −80 °C for further analysis, except for a portion of the colon tissue, which was fixed in 4% paraformaldehyde for tissue sectioning and staining. All animal experiments adhered to the Guidelines for the Care and Use of Laboratory Animals established by Hubei University of Chinese Medicine and were approved by the university's Animal Ethics Committee (permission number: SCXK 2020–0018).

Hematological Analysis

The mice were initially anesthetized using isoflurane, and blood samples were collected in EDTA-K2 anticoagulant tubes for hematological analysis. Parameters such as white blood cells (WBC), lymphocytes (LYM), and monocytes (MON) were measured with an HF-3800 hematology analyzer from Jinan Han Fang Medical Devices Co., Ltd.

Disease Activity Index (DAI) Score Analysis

During the animal experiments, body weight, stool consistency, and anal bleeding were monitored and recorded daily. The DAI scores were evaluated based on criteria outlined in the Supplementary Methods 1.

Histological Analysis

Colon tissues were fixed in 4% paraformaldehyde, dehydrated, embedded in paraffin, and sectioned into 5 μm slices. Following deparaffinization in xylene and rehydration through a gradient ethanol series, the sections were stained for histopathological examination using a hematoxylin and eosin (H&E) staining kit (Beyotime, Shanghai, China). Acidic mucins were detected via an alcian blue staining kit (Vectorlabs, Beijing, China). The production of glycosylated mucins in colon tissues was assessed through immunofluorescence using Wheat Germ Agglutinin conjugated with fluorescein isothiocyanate (WGA-FITC) (Sigma Aldrich, MO, USA). F4/80 expression was analyzed using immunohistochemistry. Photomicrographs were captured with a Leica DMIL 4000B light microscope and a Leica DFC450C digital camera (Leica Microsystems, Wetzlar, Germany).

RNA Extraction and Quantitative Real-Time PCR (RT-qPCR)

Total RNA was isolated from colon tissues using Trizol reagent. RNA (500 ng) was reverse transcribed into cDNA using the AMeasy 1st Strand cDNA Synthesis Kit (AllMEEK, Beijing, China). RT-qPCR was performed on an ABI7500 real-time PCR instrument using a 2× FastHS SYBR QPCR mixture (AllMEEK, Beijing, China). The amplification conditions were as follows: 95 °C for 10 min, followed by 40 cycles of 95 °C for 10s and 60 °C for 30s. Glyceraldehyde-3-phosphate dehydrogenase (GAPDH) was used as an internal reference for normalization, and relative gene expression was calculated using the $2(^{-\Delta\Delta Ct})$ method. Specific primer sequences are provided in Supplementary Table 1.

Western Blot

Total proteins were extracted from colon tissues using RIPA lysis buffer supplemented with a protease inhibitor cocktail (Beyotime, Shanghai, China). Protein concentration was determined using a bicinchoninic acid (BCA) protein assay kit (Beyotime, Shanghai, China). Samples were separated by sodium dodecyl sulfate-polyacrylamide gel electrophoresis (SDS-PAGE) and transferred to polyvinylidene difluoride (PVDF) membranes. After blocking with 5% skimmed milk for 1 hour, the membranes were incubated with primary antibodies overnight at 4 °C. Following washing with Tris-buffered saline containing Tween 20 (TBST), the membranes were incubated with a horseradish peroxidase (HRP)-conjugated secondary antibody (1:5000) for 1.5 hours at room temperature. After another wash, protein bands were detected using enhanced chemiluminescence (ECL) (Sigma Aldrich, MO, USA), and band densitometry was analyzed using Image J2x software (National Institutes of Health, Bethesda, MD, USA).

16S rRNA Gene Sequencing

Genomic DNA from fecal samples was extracted using the Fast DNA™ SPIN Kit (MP Biomedicals, CA, USA). The V3–V4 region of the 16S rRNA gene was amplified using primers 338F (5′-ACTCCTACGGGAGGCAGCAG-3′) and 806R (5′-GACTACHVGGGTWTCTAAT-3′), with PCR conditions of 95 °C for 5 min, followed by 20 cycles of 95 °C for 30s, 55 °C for 30s, 72 °C for 30s, and a final extension at 72 °C for 10 min. Amplicons were pooled and paired-end sequenced (2 × 300) on an Illumina MiSeq platform (Beijing Allwegene Tech, Ltd, Beijing, China), generating an average of 111,370 ± 33,990 clean reads per sample, with a minimum of 60,382 reads. Sequences were processed using QIIME, clustered into OTUs at 97% similarity, and assigned taxonomy using the SILVA database.[26] To account for differences in sequencing depth, OTU tables were rarefied to 60,000 sequences per sample before downstream alpha- and beta-diversity analyses. Ultimately, DNA samples from n=5 mice per group passed quality control and were used for subsequent sequencing analysis. Detailed analytical information can be found in the Supplementary Methods 2 and Supplementary Table 3.

Statistical Analysis

Statistical analysis was conducted using GraphPad Prism 8.0 software (La Jolla, CA, USA). The data are presented as mean ± standard error of the mean (SEM). Statistical differences were evaluated using one-way analysis of variance (ANOVA) followed by the Tukey-Kramer post hoc test. A p-value of less than 0.05 was considered statistically significant.

Results

DMY Alleviated Symptoms in Mice with DSS-Induced Colitis

Mice were administered 3% DSS to establish a model of colitis, while DMY was given via gavage for intervention. The chemical structure of DMY and the detailed experimental procedure are shown in Figure 1A and B, respectively. To assess the effects of DMY on colitis symptoms, we monitored changes in body weight daily. Mice in the DSS group experienced continuous weight loss ($p < 0.01$ vs Ctrl group), while DMY administration did not significantly reverse this weight loss ($p > 0.05$ vs DSS group) (Figure 1C). Additionally, mice with DSS-induced colitis exhibited typical symptoms such as diarrhea and hematochezia, leading to a progressive increase in the Disease Activity Index (DAI) score. Medium-to-high doses of DMY reduced the DAI score by day 7 ($p < 0.01$ vs DSS group) (Figure 1D). In terms of colon length, the DSS group presented a shorter colon ($p < 0.01$ vs Ctrl group), and this change was not improved by DMY intervention (Figure 1E and F).

The spleen, an important immune organ, showed considerable enlargement in the DSS group ($p < 0.01$ vs Ctrl group). Medium-dose DMY administration statistically reduced the spleen index ($p < 0.05$ vs DSS group) (Figure 1G). Similarly, pro-inflammatory cytokines IL-1β and IL-6 were elevated in the plasma of colitis mice ($p < 0.05$ or 0.01 vs Ctrl group). Although high doses of DMY reduced these cytokine levels, the effect was not statistically significant (Figure 1H). Hematological analyses revealed a significant increase in white blood cell (WBC) count in colitis mice ($p < 0.01$ vs Ctrl group), particularly among lymphocytes (LYM) and monocytes (MON). DMY treatment reduced the counts of these blood cells in a dose-dependent manner ($p < 0.05$ or 0.01 vs DSS group) (Figure 1I–K).

DMY Repaired Intestinal Barrier Damage in in Mice with DSS-Induced Colitis

Damage to the intestinal barrier disrupts intestinal homeostasis in colitis.[27] H&E staining revealed that the colonic mucosal layer was damaged in the DSS group, showing destruction of villus and crypt structures, along with massive infiltration of inflammatory cells. This damage was partially reversed by DMY intervention (Figure 2A). Histological scoring was performed based on Supplementary Table 2, and the result indicated that DMY reduced the score in colitis mice ($p < 0.01$ vs DSS group) (Figure 2B). The colonic mucus layer is composed of gelatinous, highly glycosylated proteins secreted by goblet cells. As demonstrated by Alcian Blue staining and WGA-FITC staining, DMY notably increased the levels of glycosylated and acidic mucins in colitis mice ($p < 0.01$ vs DSS group) (Figure 2C and D). Moreover, the mRNA expression of tight junction proteins and mucins in colon tissues was measured. Figure 2E–G

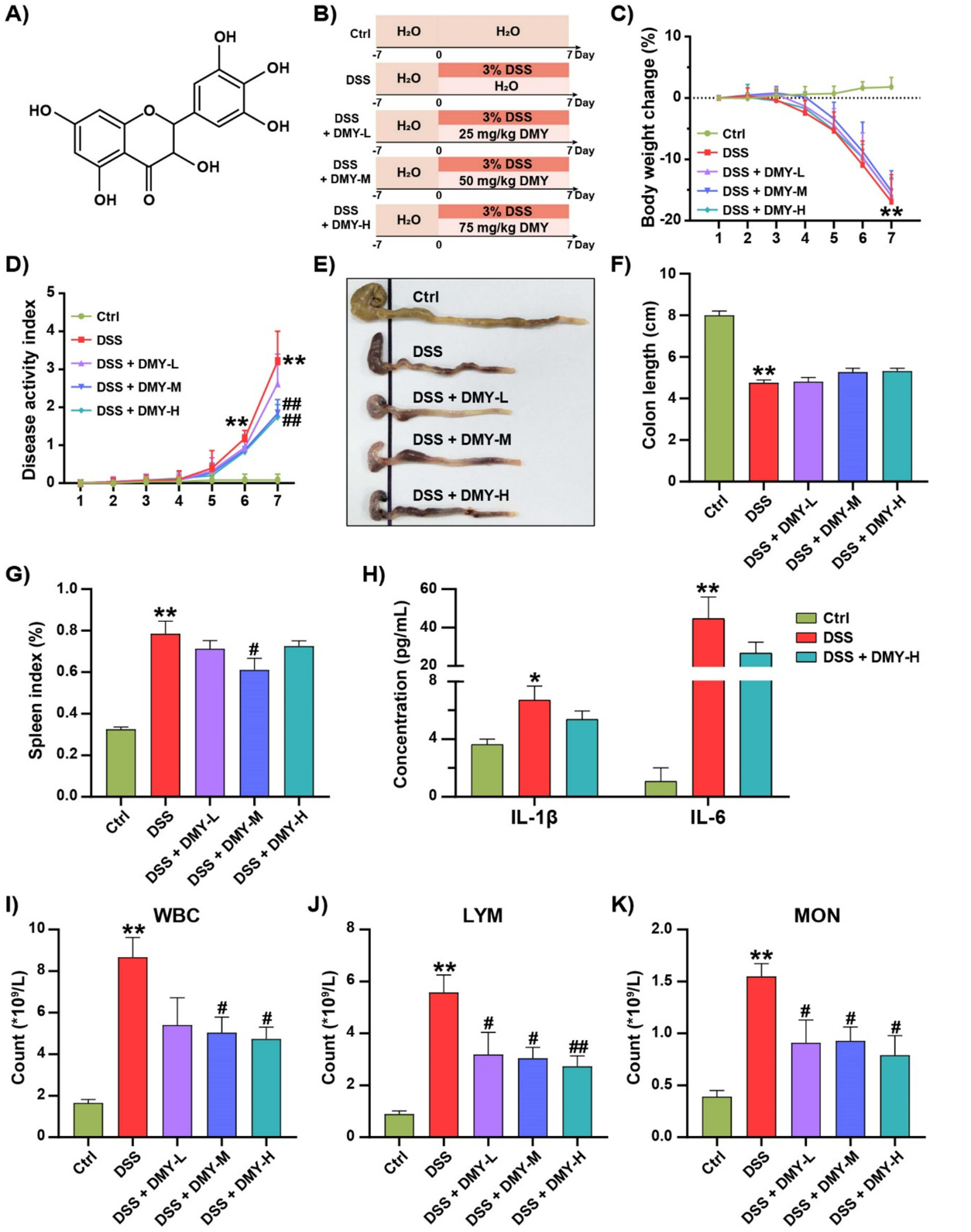

Figure 1 DMY improved physicochemical parameters in mice with DSS-induced colitis. (**A**) Chemical structure of DMY. (**B**) Experimental schedule. (**C**) Percentage changes in body weight during the disease progression. (**D**) Disease Activity Index (DAI). (**E**) Representative photograph of the colon. (**F**) Colon length. (**G**) Spleen index. (**H**) Plasma levels of IL-1β and IL-6. (**I**) White blood cell (WBC) count. (**J**) Lymphocyte (LYM) count. (**K**) Monocyte (MON) count. Data are presented as mean ± SEM (n=8). $^{*}p < 0.05$ and $^{**}p < 0.01$ vs Ctrl group; $^{\#}p < 0.05$ and $^{\#\#}p < 0.01$ vs DSS group.

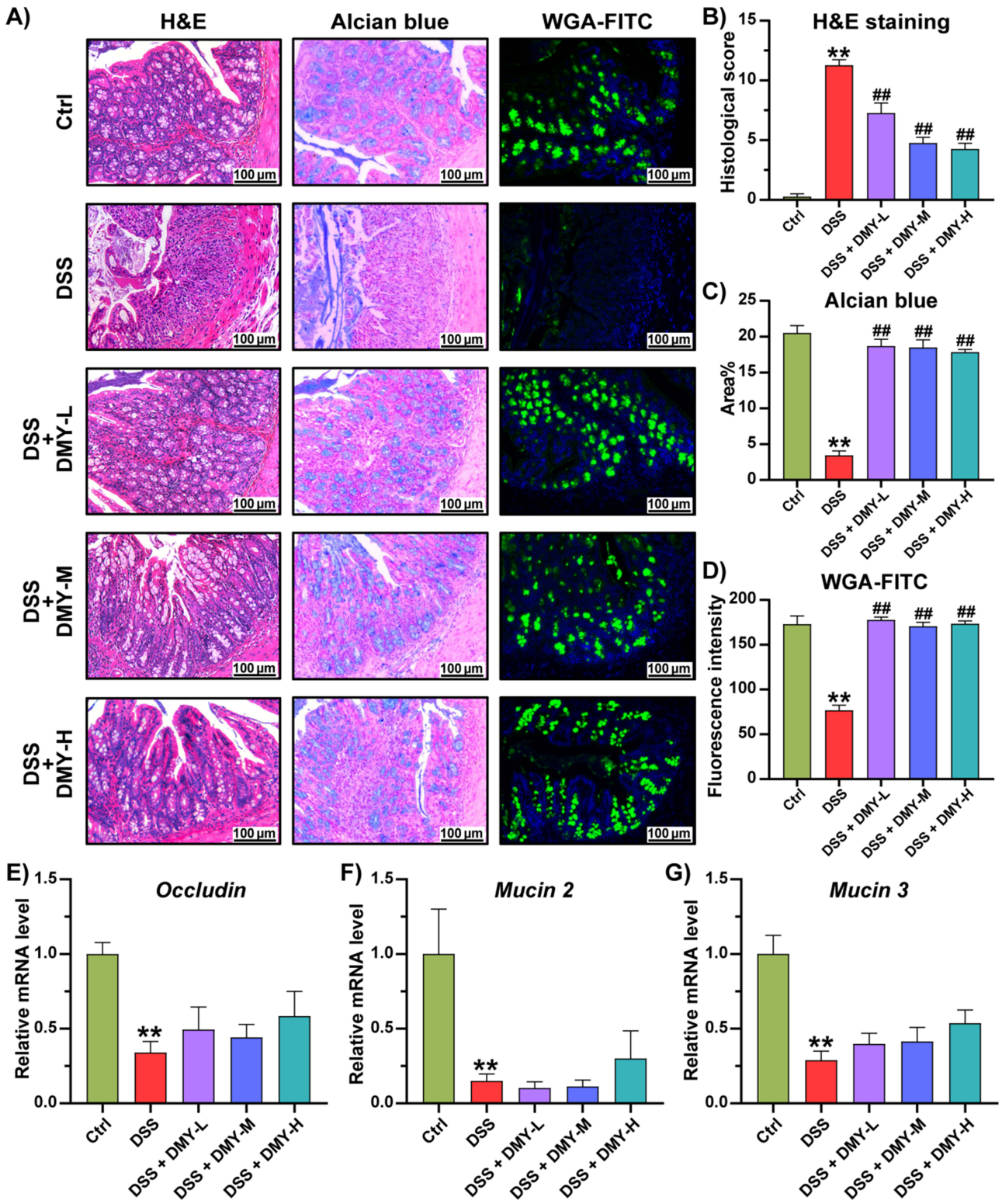

Figure 2 DMY protected the intestinal barrier in mice with DSS-induced colitis. (**A**) Morphological analysis of colon tissues by hematoxylin and eosin (H&E) staining, Alcian blue staining, and fluorescein isothiocyanate-conjugated wheat germ agglutinin (WGA-FITC) staining (scale bar = 100 μm, magnification of the microphotograph, × 200). (**B**) Histological score. (**C**) Quantification of the area stained with Alcian blue. (**D**) Quantification of the fluorescence intensity from WGA-FITC staining. (**E**–**G**) Relative mRNA levels of *Occludin* (**E**), *Mucin 2* (**F**), and *Mucin 3* (**G**) in colon tissues. Data are presented as mean ± SEM (n=8). $^{**}p < 0.01$ vs Ctrl group; $^{\#\#}p < 0.01$, vs DSS group.

https://doi.org/10.2147/JIR.S545159

showed that DMY increased the levels of *Occludin, Mucin 2*, and *Mucin 3* in the colon tissues of colitis mice, although these differences were not statistically significant. In summary, these results suggested that DMY was effective in repairing intestinal barrier damage in mice with DSS-induced colitis.

DMY Improved Gut Microbiota Dysbiosis in Mice with DSS-Induced Colitis

The maintenance of gut homeostasis relies on a diverse and complex microbial community.[28] When the intestinal barrier is compromised, disturbances in the gut microbiota often occur. To investigate the effect of DMY on gut microbiota in colitis mice, we conducted 16S rRNA sequencing to profile the structure of the gut microbiota, focusing on the V3-V4 variable region. We assessed the α-diversity of the gut microbiota using the Chao1 index and the Observed species index. Our results indicated that α-diversity was reduced in the DSS group ($p < 0.01$ vs Ctrl group). Following DMY treatment, α-diversity showed partial restoration, though this difference was not statistically significant (Figure 3A and B). We conducted a PERMANOVA analysis based on the Bray-Curtis distance matrix, which yielded a Pseudo-F statistic of 8.3 and a p-value of 0.001. The Ctrl, DSS, and DSS + DMY groups were classified into distinct clusters in the non-metric multidimensional scaling (NMDS) and principal component analysis (PCA) plots, highlighting that these three experimental groups had different gut microbiota structures (Figure 3C and D).

Next, we quantified the relative abundance of gut microbiota. At the phylum level, we found a reduction in the relative abundance of Bacteroidota and an increase in Deferribacterota in the DSS group. DMY treatment reversed these changes (Figure 3E). At the family level, DMY decreased the abundance of Desulfovibrionaceae and Erysipelotrichaceae in DSS-induced colitis mice while increasing the abundance of Muribaculaceae (Figure 3F). At the genus level, we conducted a heatmap analysis to identify bacteria with significant changes in abundance. As illustrated in Figure 3G, *Turicibacter, Clostridium sensu stricto 1*, and *Desulfovibrio* were markedly increased in the DSS group, whereas *Parabacteroides, Muribaculum*, and *Lachnospiraceae NK4A136 group* were significantly decreased. Notably, DMY treatment reversed these alterations at the genus level ($p < 0.05$, vs DSS group).

To further identify characteristic bacterial taxa, we employed linear discriminant analysis effect size (LEfSe). We discovered eleven specific bacterial taxa in the Ctrl group, fourteen in the DSS group, and thirteen in the DSS + DMY group (Figure 3H). Additionally, we performed linear discriminant analysis (LDA) to highlight the bacterial taxa with the most significant differences in abundance (Figure 3I): 1) f_Muribaculaceae, p_Bacteroidota, c_Bacteroidia, o_Bacteroidales, and f_Prevotellaceae for Ctrl group; 2) f_Erysipelotrichaceae, o_Erysipelotrichales, *g_Bacteroides*, f_Bacteroidaceae, and s_Bacteroides acidifaciens JCM 10556 for DSS group; 3) p_Proteobacteria, c_Gammaproteobacteria, *g_Escherichia Shigella*, o_Enterobacterales, and f_Enterobacteriaceae for DSS + DMY group.

DMY Modulated Intestinal Immune Dysregulation in Mice with DSS-Induced Colitis

Intestinal barrier damage and microbiota dysbiosis can accelerate the excessive activation of intestinal immune cells and the release of pro-inflammatory factors, disrupting intestinal homeostasis.[29] Next, we assessed the mRNA levels of inflammatory cytokines in the colon tissues of DSS-induced colitis mice using RT-qPCR. As shown in Figure 4A, DMY treatment inhibited the mRNA expression of Tumor necrosis factor-α (*Tnf-α*), Interleukin-6 (*Il-6*) and Cyclooxygenase-2 (*Cox-2*) in a dose-dependent manner ($p < 0.05$ or 0.01 vs DSS group). A more pronounced suppression was observed at the medium dose of DMY for C-X-C Motif Chemokine Ligand 1 (*Cxcl1*) and C-X-C Motif Chemokine Ligand 10 (*Cxcl10*) ($p < 0.05$ or 0.01 vs DSS group).

Similarly, DMY effectively reduced the high expression of Inducible nitric oxide synthase (iNOS), Myeloperoxidase (MPO), and COX-2 at the protein level in the colon tissues of colitis mice ($p < 0.01$ vs DSS group) (Figure 4B and C). Additionally, the MAPK signaling pathway was activated in colitis mice. DMY treatment decreased the protein expression of p-ERK and p-JNK ($p < 0.05$ or 0.01 vs DSS group) (Figure 4D and E). Immunohistochemical staining of F4/80 in colon tissues revealed an increase in the number of positive macrophages in the DSS group. Macrophage infiltration was alleviated following DMY treatment (Figure 4F).

The NLRP3 inflammasome plays a critical regulatory role in immune responses. Studies have confirmed that the formation and excessive activation of the NLRP3 inflammasome contribute to the development of colitis.[30] Therefore, our study also focused on the NLRP3 inflammasome. We found that DMY significantly reduced the mRNA levels of

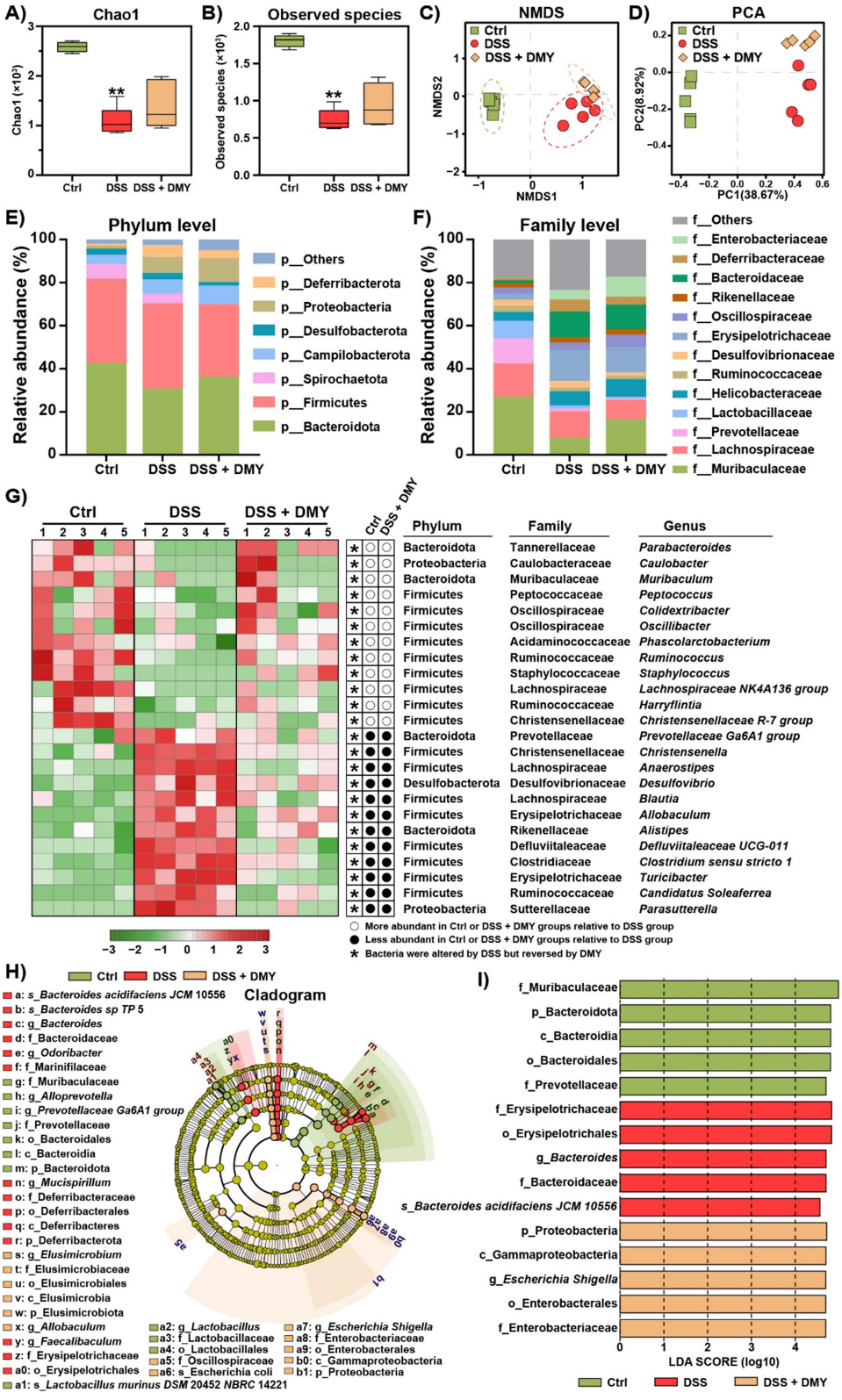

Figure 3 DMY illustrates how the composition and structure of gut microbiota were altered in mice with DSS-induced colitis. (**A** and **B**) Alpha diversity of the gut microbiota was evaluated using the Chao1 index (**A**) and the observed species index (**B**). (**C**) Non-metric multidimensional scaling (NMDS) analysis. (**D**) Principal component analysis (PCA). (**E**) Changes in gut microbiota composition at the phylum level. (**F**) Alterations in gut microbiota composition at the family level. (**G**) Relative abundance of gut microbiota at the genus level determined by heatmap analysis. (**H**) Characteristic taxa among the experimental groups were identified using linear discriminant analysis effect size (LEfSe). (**I**) A linear discriminant analysis (LDA) score greater than 4 indicated a higher abundance in the corresponding group compared to the other groups. Data are presented as mean ± SEM (n=5).

https://doi.org/10.2147/JIR.S545159

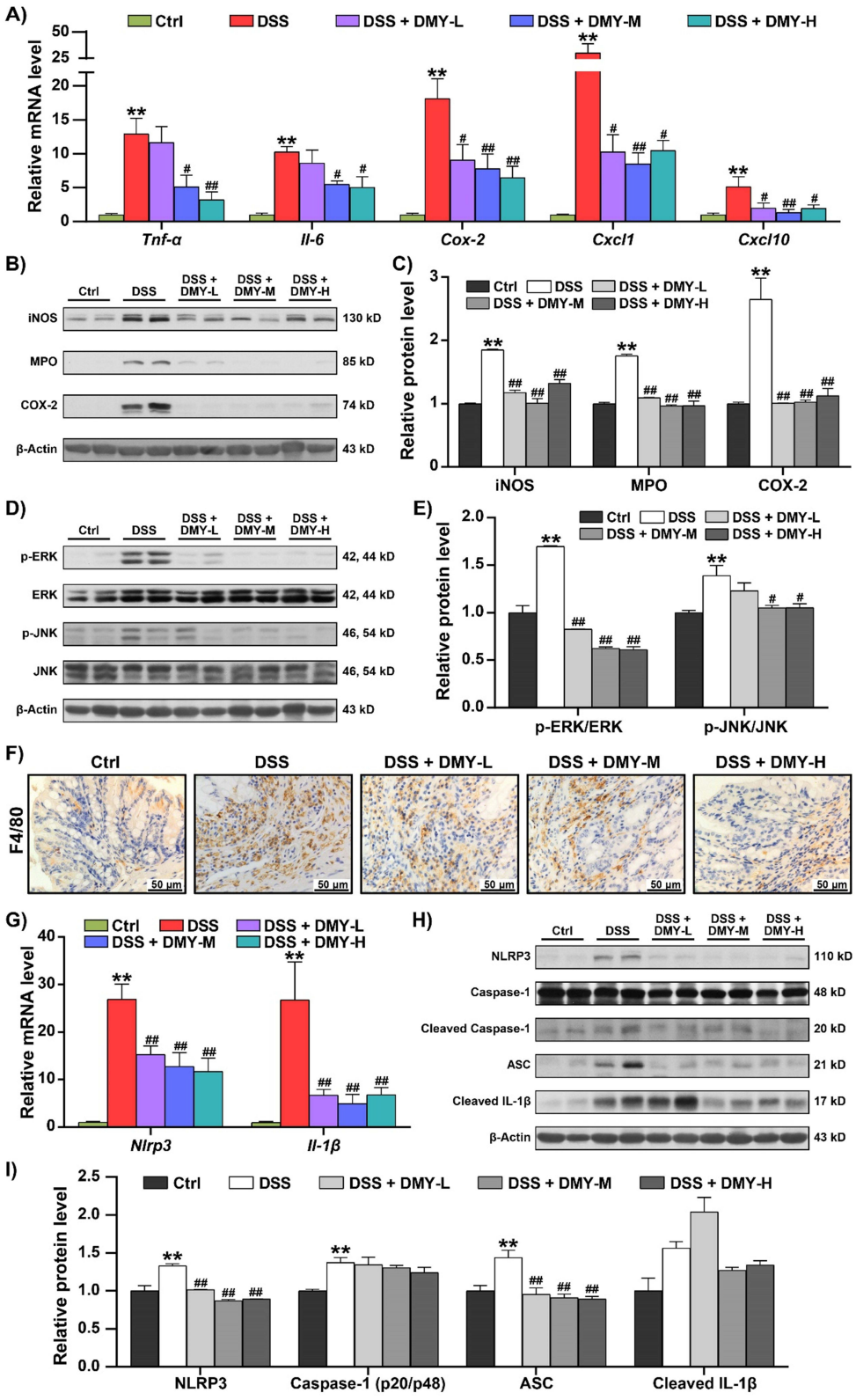

Figure 4 DMY inhibited abnormal immune response in the colon of mice with DSS-induced colitis. (**A**) mRNA levels of inflammatory cytokines, including *Tnf-α, Il-6, Cox-2, Cxcl1*, and *Cxcl10*, were measured using RT-qPCR. (**B**) Protein expressions of iNOS, MPO, and COX-2 in colon tissues were analyzed by Western blot. (**C**) Relative protein intensities of iNOS, MPO, and COX-2. (**D**) Protein expressions of p-ERK, ERK, p-JNK, and JNK in colon tissues were assessed by Western blot. (**E**) Relative protein intensities of p-ERK and p-JNK. (**F**) Immunohistochemical analysis of F4/80 in colon tissues (scale bar = 50 μm, magnification of the microphotograph, ×400). (**G**) Relative mRNA levels of *Nlrp3* and *Il-1β* in colon tissues. (**H**) Protein expressions of NLRP3, Cleaved Caspase-1, ASC and Cleaved IL-1β in colon tissues. (**I**) Relative protein intensities of NLRP3, Cleaved Caspase-1, ASC and Cleaved IL-1β. Data are presented as mean ± SEM (n=8). $^{**}p < 0.01$ vs Ctrl group; $^{\#}p < 0.05$ and $^{\#\#}p < 0.01$, vs DSS group.

Nlrp3 and Interleukin-1β (*Il-1β*) in the colon tissues of DSS-induced colitis mice ($p < 0.01$ vs DSS group) (Figure 4G). Western blot analysis further demonstrated that DMY markedly suppressed the protein expression of NLRP3 and Apoptosis-Associated Speck-Like Protein Containing a CARD (ASC) ($p < 0.01$ vs DSS group). Although DMY showed a downward trend in the protein levels of Cleaved Caspase-1 and Cleaved IL-1β, the differences were not statistically significant (Figure 4H and I).

NLRP3 Was a Critical Target for DMY in Modulating Inflammatory Response in Mice with DSS-Induced Colitis

To confirm whether NLRP3 was a key target for DMY in alleviating intestinal inflammation, we utilized *Nlrp3* knockout mice. First, we verified the successful knockout of the *Nlrp3* gene in all experimental mice (Supplementary Figure S1) and established a colitis model using 3% DSS with the *Nlrp3* knockout mice. Detailed animal experimental procedures are illustrated in Figure 5A. After knocking out *Nlrp3*, DMY treatment did not alleviate the symptoms of DSS-induced colitis. This was evidenced by observations of body weight (Figure 5B), DAI score (Figure 5C and D), colon length (Figure 5E and F), and spleen index (Figure 5G). Furthermore, all three groups of DSS-induced colitis mice showed similar damage to the intestinal barrier structure. Histological analysis also revealed no improvement in the structural damage of intestinal crypts, the infiltration of inflammatory cells, or the reduction of glycosylated and acidic mucins, as assessed by H&E, Alcian Blue, and WGA-FITC staining (Figure 5H–K).

We further validated the key role of NLRP3 at the protein level. As shown in Figure 6A and B, DMY was unable to suppress the increase in inflammatory proteins, such as iNOS, MPO, and COX-2, in the intestinal tissues of *Nlrp3* knockout mice with colitis. Additionally, we examined changes in the NLRP3 inflammasome. Our results indicated that DMY did not inhibit the expression of cleaved Caspase-1, ASC, or cleaved IL-1β in the intestines of DSS-induced *Nlrp3* knockout colitis mice (Figure 6C and D).

Building on these observations, we conducted Spearman correlation analysis to explore the relationships between *Nlrp3, IL-1β*, and indicators related to intestinal homeostasis in mice, including gut microbiota, intestinal barrier function, and the immune response. As indicated in Figure 6E, *Nlrp3* and *IL-1β* were positively correlated with harmful gut bacteria, such as *Clostridium sensu stricto 1* and *Turicibacter*, as well as intestinal inflammatory cytokines ($p < 0.01$). In contrast, they were negatively correlated with beneficial gut bacteria, such as *Prevotellaceae UCG-001* and *Faecalibacterium*, and with intestinal barrier function ($p < 0.05$ or 0.01). These findings further support the hypothesis that the remission of colitis induced by DMY, mediated through the NLRP3 inflammasome, may also be closely related to changes in the gut microbiota.

Gut Microbiota Is a Crucial Mediator in the Alleviation of DSS-Induced Colitis by DMY

In the study mentioned above, we first observed that the alleviating effect of DMY on DSS-induced colitis in mice is closely related to *Nlrp3*. Further analysis revealed a connection between *Nlrp3* activity and the gut microbiota, leading us to conduct an in-depth investigation into their interrelationship and underlying mechanisms.

To confirm the critical role of the gut microbiota, we treated mice with an antibiotic cocktail for eight weeks to establish a pseudo-germ-free mouse model. Colitis was then induced in these mice using 3% DSS, and DMY intervention was administered starting at week nine (Figure 7A). The gut microbiota of the mice was quantified using RT-qPCR (primer sequences are provided in Supplementary Table 4). The results showed significant reductions in the overall gut microbiota as well as in specific bacterial populations, such as Bacteroides and Bifidobacteria, in the intestines of mice treated with the antibiotic cocktail (Supplementary Figure S2). Compared to the DSS group, DMY treatment did not improve physiological indices, including body weight, DAI score, colon length, and spleen index, in colitis mice with depleted gut microbiota (Figure 7B–G). Additionally, histological scores and H&E staining results confirmed that DMY intervention failed to restore the structural integrity of intestinal tissues in these mice (Figure 7H and I).

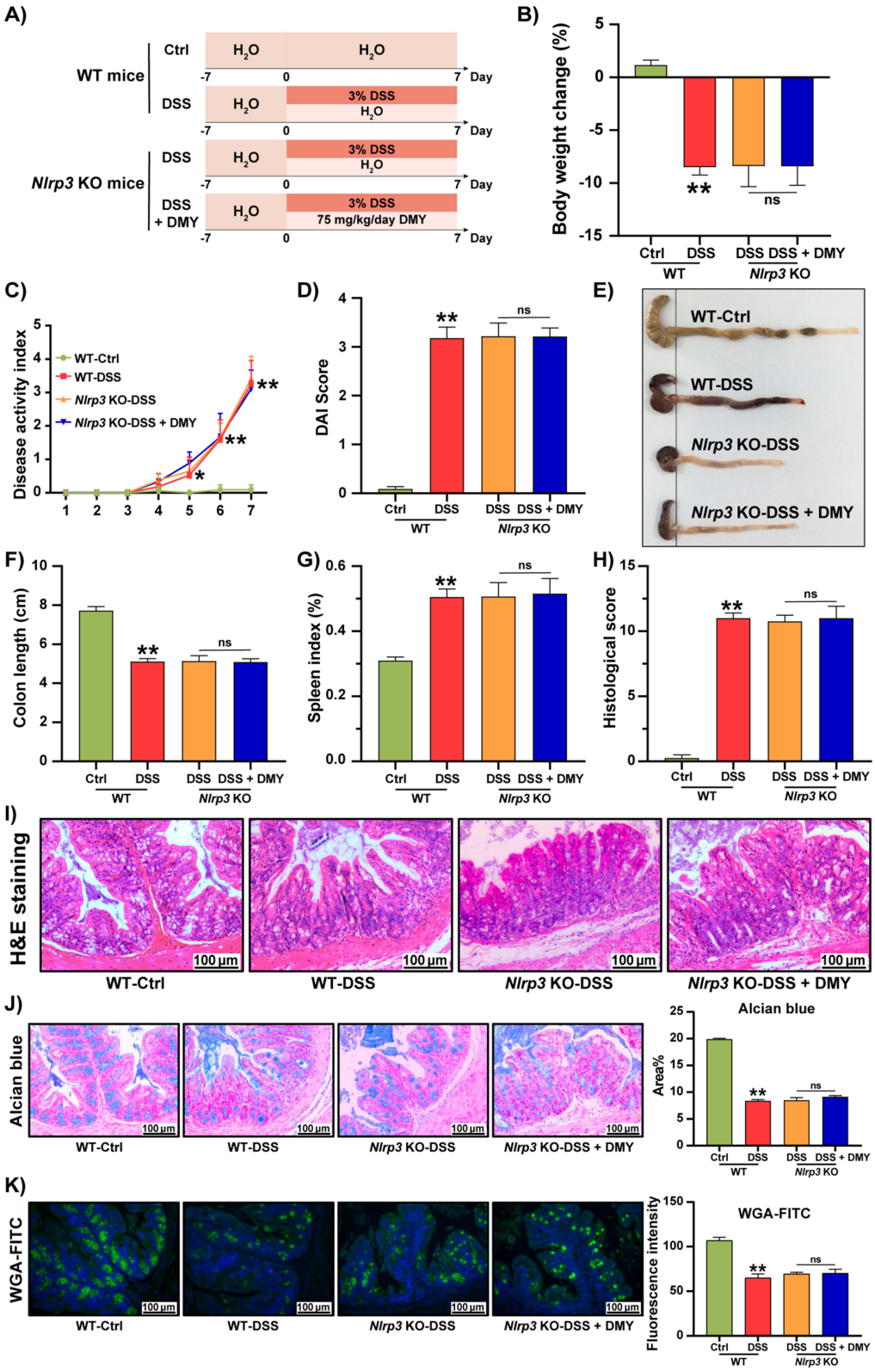

Figure 5 DMY failed to regulate physiological indices and intestinal barrier function in *Nlrp3* KO mice with DSS-induced colitis. (**A**) Experimental schedule. (**B**) Body weight changes of the mice at the end of the experiment. (**C**) DAI score curve. (**D**) DAI scores of the mice at the end of the experiment. (**E**) Photographs of the colon. (**F**) Colon length. (**G**) Spleen index. (**H**) Histological score. (**I**) Morphological analysis of colon tissues by H&E staining (scale bar = 100 μm, magnification of the microphotograph, × 200). (**J**) Alcian blue staining of colon tissues is shown along with area quantification (scale bar = 100 μm, magnification of the microphotograph = 200×). (**K**) WGA-FITC staining of colon tissues is presented alongside fluorescence intensity quantification (scale bar = 100 μm, magnification of the microphotograph = 200×). Data are presented as mean ± SEM (n=8). **p* < 0.05 and ***p* < 0.01 vs WT-Ctrl group.

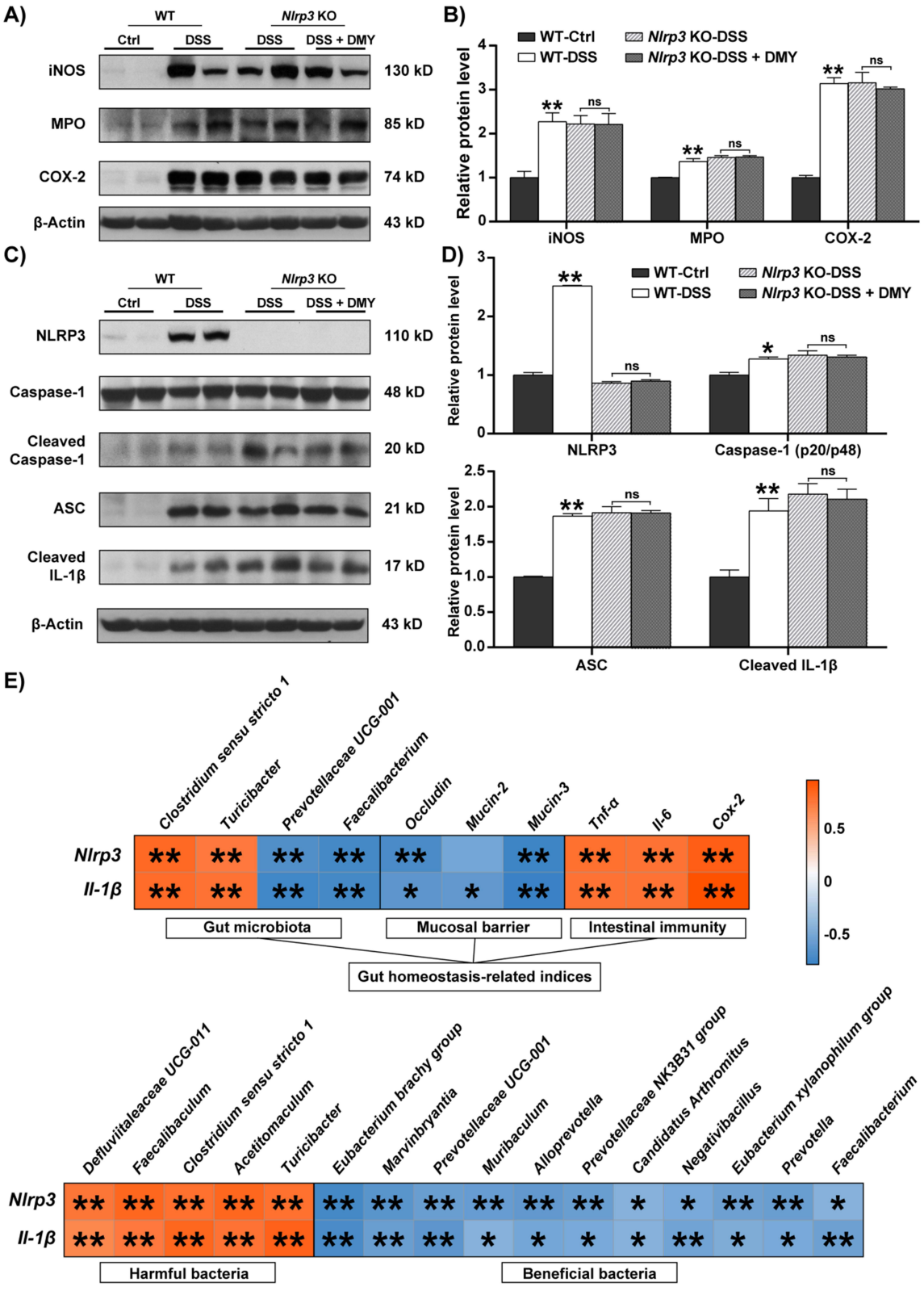

Figure 6 DMY failed to inhibit intestinal inflammation in *Nlrp3* KO mice with DSS-induced colitis. (**A**) Protein expression levels of iNOS, MPO, and COX-2 in colon tissues. (**B**) Relative protein intensities of iNOS, MPO and COX-2. (**C**) Protein expression levels of NLRP3, Cleaved Caspase-1, ASC, and Cleaved IL-1β in colon tissues. (**D**) Relative protein intensities of NLRP3, Cleaved Caspase-1, ASC and Cleaved IL-1β at protein levels. (**E**) Spearman correlation analysis between *Nlrp3, Il-1β*, and indicators related to gut homeostasis, including gut microbiota, intestinal barrier function, and inflammation levels. Additionally, the correlation between *Nlrp3, IL-1β*, and changes at the genus level of gut microbiota was presented. The color scale ranged from blue (negative correlation) to Orange (positive correlation). Data are presented as mean ± SEM. *$p < 0.05$ and **$p < 0.01$ vs Ctrl group.

https://doi.org/10.2147/JIR.S545159

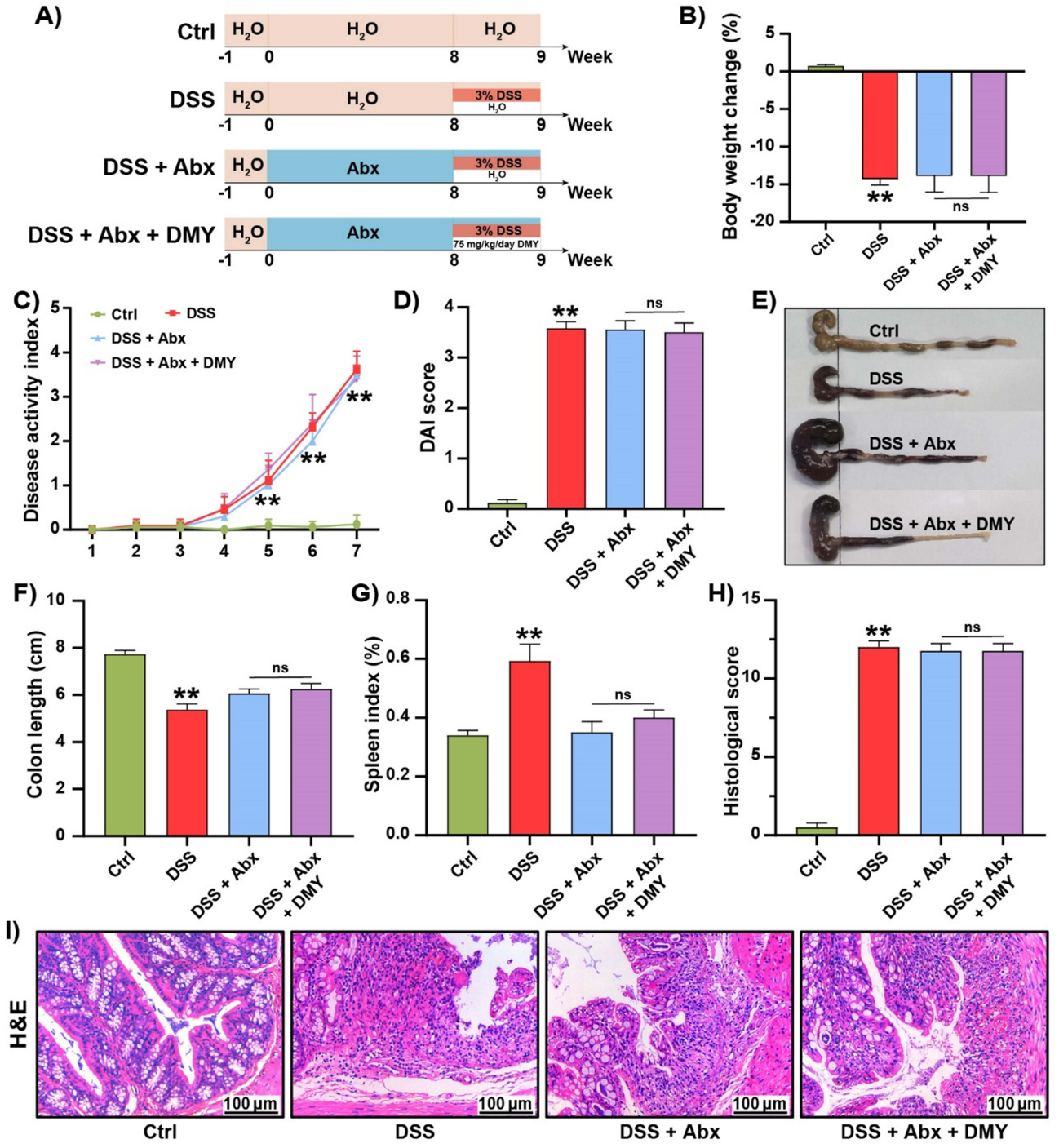

Figure 7 DMY did not improve physiological indices or prevent intestinal damage in DSS-induced pseudo-germ-free mice. (**A**) Experimental schedule. (**B**) Change in body weight percentage of mice at the end of the experiment. (**C**) Disease Activity Index (DAI) score curves throughout the experiment. (**D**) DAI scores at the end of the experiment. (**E**) Images of colon tissues. (**F**) Colon length measurements. (**G**) Spleen index. (**H**) Histologic score. (**I**) Morphological analysis of colon tissues by H&E staining (scale bar = 100 μm, magnification of the microphotograph, × 200). Data are presented as mean ± SEM (n=8). $^{**}p < 0.01$ vs Ctrl group.

Inhibition of NLRP3 by DMY Was Modulated by Gut Microbiota

Staining of colon tissues with Alcian blue and WGA-FITC indicated that DMY did not restore the reduced intestinal mucin content in colitis mice with depleted gut microbiota (Figure 8A–D). To further investigate the role of gut microbiota in maintaining intestinal homeostasis, we examined the changes in the NLRP3 inflammasome at the protein level in pseudo-germ -free colitis mice. As shown in Figure 8E and F, DMY was unable to down-regulate the expression of NLRP3, ASC, and

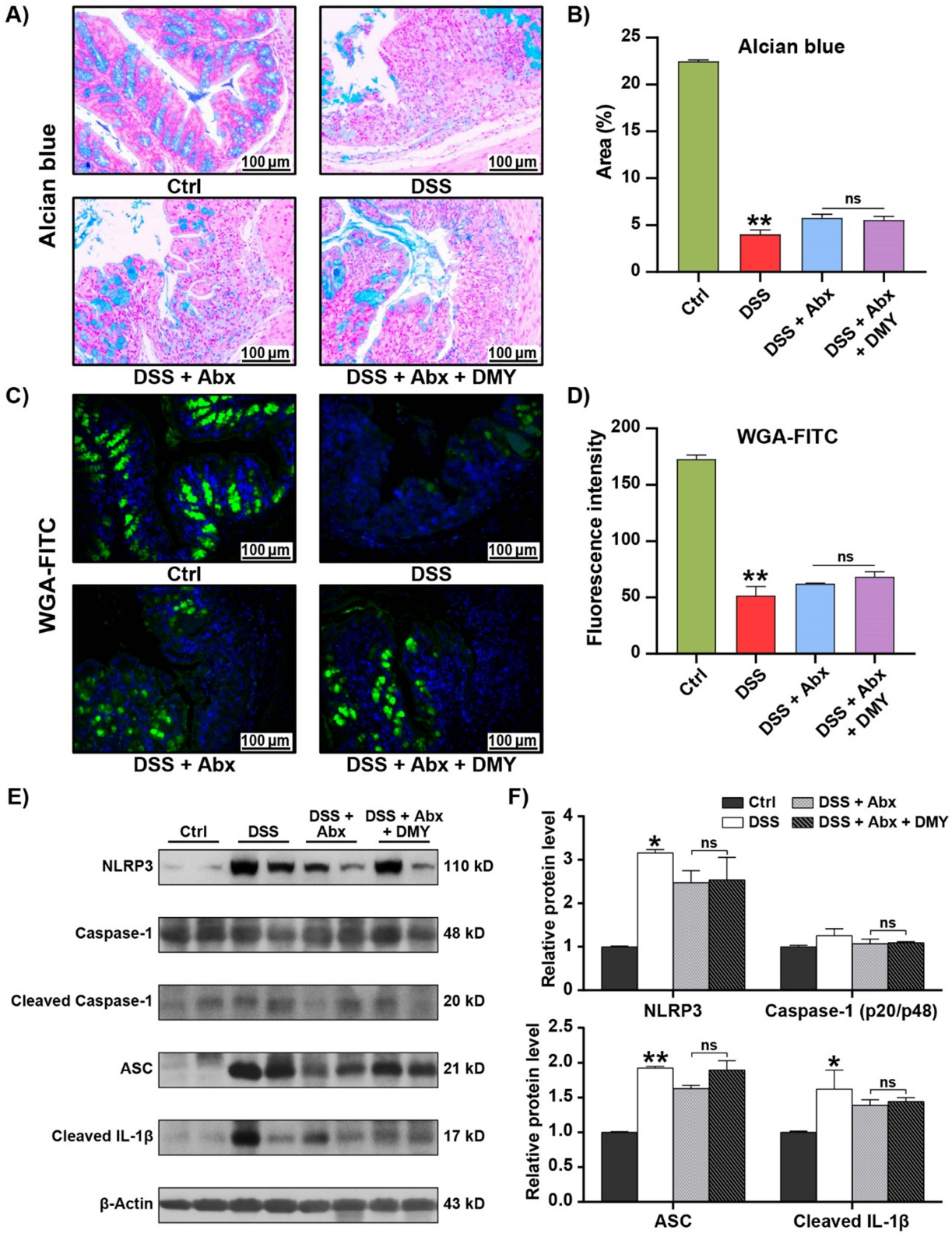

Figure 8 DMY did not improve intestinal barrier function and inflammation in DSS-induced pseudo-germ-free mice. (**A**) Morphological analysis of colon tissues using Alcian blue staining (scale bar = 100 μm, magnification of the microphotograph, ×200). (**B**) Quantification of the area stained by Alcian blue. (**C**) Morphological analysis of colon tissues using WGA-FITC staining (scale bar = 100 μm, magnification of the microphotograph, ×200). (**D**) Quantification of fluorescence intensity of WGA-FITC staining. (**E**) Protein expression levels of NLRP3, Cleaved Caspase-1, ASC, and Cleaved IL-1β in colon tissues. (**F**) Relative intensities of NLRP3, Cleaved Caspase-1, ASC, and Cleaved IL-1β at the protein level. Data are presented as mean ± SEM (n=8). *$p < 0.05$ and **$p < 0.01$ vs Ctrl group.

https://doi.org/10.2147/JIR.S545159

Cleaved IL-1β. These results suggest that the inhibitory effect of DMY on the NLRP3 inflammasome is lost after gut microbiota depletion.

Discussion

Tea culture in China has a history of millennia, with tea varieties primarily classified into three categories: green tea, oolong tea, and black tea.[31] In addition, several traditional Chinese medicines, such as vine tea and *Ligustrum robustum (Roxb.) blume*, are used to create tea beverages that are believed to offer health benefits and disease-preventive properties.[32] Notably, vine tea, known as the "King of Flavonoids," contains a high concentration of DMY, its predominant bioactive compound.[33] DMY has been shown to exhibit a range of pharmacological activities, including alleviating colitis in mice. This study further investigated the regulatory mechanisms of DMY on the mucosal barrier, gut microbiota, and immune response, demonstrating that DMY plays a key role in restoring intestinal homeostasis. This restoration was associated with a reduced risk of disease recurrence and provided long-lasting protection, thereby enhancing the overall therapeutic outcomes. These findings provide strong evidence for the beneficial protective effects of DMY on the gastrointestinal system.

The DSS-induced mouse model is widely used for modeling colitis due to its simplicity and the close resemblance of its symptoms to those observed in human colitis.[34] In this study, DSS-treated mice exhibited typical colitis symptoms, including weight loss, diarrhea, bloody stools, and colon shortening.[35] Although DMY treatment did not significantly improve weight loss or colon shortening, it effectively reduced the severity of diarrhea and bloody stools, leading to a lower DAI score (Figure 1C–F). Colitis pathogenesis is characterized by dysregulated immune responses and inflammatory pathways, often involving immune imbalance and leukocyte recruitment.[36] The spleen, a key immune organ, commonly enlarges during infection or inflammation, which is reflected by an increased spleen index.[37] Our results demonstrated that DMY effectively reduced the spleen index in colitis mice (Figure 1G). Additionally, ELISA and hematological analysis revealed that DMY exerted significant anti-inflammatory effects in colitis mice (Figure 1H–K). The limited improvements in body weight and colon length may reflect dissociation between macroscopic tissue damage and underlying inflammatory signaling. While these larger, more visible parameters may not fully recover, DMY could still exert significant effects at the molecular or cellular level, particularly in modulating inflammation and reshaping the gut microbiota. Specifically, the structural recovery of colon length and the restoration of body weight may lag behind the resolution of systemic and local inflammation, which may account for the observed phenomenon in the acute model following short-term intervention.

The disruption of the intestinal mucosal barrier is considered a pivotal early event in the pathogenesis of colitis.[38] This barrier is primarily composed of the epithelial cell layer, tight junction proteins, and the mucus layer, which together play a critical role in preventing pathogen invasion and maintaining intestinal homeostasis.[39] When the integrity of this barrier is compromised or lost, gut bacteria and pathogens can penetrate the epithelial layer, triggering an immune response that exacerbates inflammation and ultimately leads to the development of colitis.[40] Our experimental results demonstrated that DMY significantly alleviated the structural damage to crypts, inflammatory cell infiltration, and reduction of mucin in the colonic tissue of colitis mice (Figure 2), effectively protecting the intestinal mucosal barrier and restoring intestinal homeostasis. These effects are consistent with reports showing that nutrients and phytochemicals can promote intestinal mucosal healing by regulating macrophage-mediated immune responses,[41] supporting the idea that DMY's protective effect extends beyond immune suppression to actively restoring the mucosal barrier.

The gut microbiota, which predominantly resides in the mucus layer, is integral to maintaining gut health.[42] Under physiological conditions, the microbiota plays a crucial role in safeguarding intestinal homeostasis by promoting barrier function, modulating immune responses, competitively inhibiting pathogenic microorganisms, and regulating gut metabolism.[43] Additionally, alterations in the composition and diversity of the gut microbiota have been implicated as potential biomarkers of colitis and other intestinal disorders.[44] There exists a symbiotic relationship between the gut microbiota and the intestinal barrier, where the microbiota not only supports the structural integrity of the barrier but also facilitates immune modulation and the overall functionality of the gut through the production of metabolites.[45] In the present study, we observed that DMY treatment led to a significant increase in the diversity of the gut microbiota in colitis mice (Figure 3A–D). Notably, Bacteroidota, the most abundant phylum in the gut, is known to exert beneficial

effects on host health,[46] and DMY treatment effectively reversed its depletion (Figure 3E). Furthermore, DMY improved the aberrant changes in the relative abundances of Desulfovibrionaceae and Muribaculaceae at the family level, which are typically characterized as harmful and beneficial bacterial families, respectively (Figure 3F).[47,48] Previous studies have demonstrated that a loss of beneficial taxa alongside an expansion of pro-inflammatory bacteria contributes to intestinal disorders,[49] emphasizing the pivotal role of microbial composition in colitis pathogenesis.

The inflammasome plays a central role in innate immune responses, enabling the body to react to infections and tissue injury by inducing inflammation. This inflammatory response not only helps to eliminate pathogens but also facilitates tissue repair, ultimately restoring homeostasis.[50] Specifically, the NLRP3 inflammasome is assembled through the interaction of NLRP3 with ASC and pro-caspase-1, leading to the activation of caspase-1. This activation, in turn, promotes the maturation and secretion of the pro-inflammatory cytokines IL-1β and IL-18, which are critically involved in the pathogenesis of colitis.[51,52] Recent advances in the field have highlighted the potential of small-molecule inhibitors targeting the NLRP3 inflammasome. These inhibitors, by acting directly or indirectly on this multiprotein complex, have shown promise in mitigating pathological processes in various preclinical disease models.[53] However, to date, few studies have explored the relationship between the NLRP3 inflammasome and DMY in the context of colitis. In our study, we observed significant activation of the NLRP3 inflammasome in the colitis mouse model, which was effectively suppressed by DMY treatment (Figure 4G–I). Furthermore, colitis mice with *Nlrp3* knockout exhibited pronounced weight loss, increased disease activity index, shortened colon length, and elevated spleen index. Pathological features, including colon tissue damage and reduced mucin production, persisted despite DMY treatment (Figure 5). Additional analysis revealed that DMY treatment did not significantly inhibit the expression of inflammatory proteins in intestinal tissues (Figure 6A–D). This underscored the possibility that suppression of the NLRP3 inflammasome was a critical mechanism underlying DMY's anti-colitis effects. Further correlation analysis showed that the expression levels of *Nlrp3* and *Il-1β* were either positively or negatively correlated with altered gut microbiota profiles in colitis mice (Figure 6E). Based on these findings, we proposed that the gut microbiota may play a significant role in the pathway through which DMY ameliorated colitis by inhibiting the NLRP3 inflammasome.

In the acute DSS model employed in this study, while DMY significantly inhibited NLRP3 inflammasome activation and improved systemic inflammation markers (eg, peripheral blood leukocyte count), its effects on the restoration of certain macroscopic phenotypes, such as colon length, were limited. The pathogenesis of UC is complex, involving multiple parallel signaling pathways (such as NF-κB, JAK-STAT, etc.) and long-term tissue remodeling. Thus, the potent inhibition of the NLRP3 inflammasome alone may not be sufficient to fully reverse all pathological damage in the short term. Therefore, future therapeutic strategies might consider combining NLRP3-specific inhibitors like DMY with other therapies that target different signaling pathways or promote mucosal repair, with the goal of achieving more comprehensive therapeutic outcomes.

Recent studies have highlighted other natural products, such as curcumin and resveratrol, which also target the NLRP3 inflammasome or gut microbiota to alleviate inflammation in various disease models.[54–56] In line with studies showing that natural compounds can modulate gut microbiota and immune responses,[57] DMY demonstrates a unique dual-target effect on both the NLRP3 inflammasome and microbial composition, providing a more comprehensive therapeutic potential. In contrast to these compounds, which primarily focus on either inflammation or microbiota modulation, DMY appears to address both aspects in a synergistic manner. This unique dual-target mechanism positions DMY as a promising natural therapeutic candidate for colitis and other inflammatory diseases.

Reduced diversity, altered composition, and disrupted spatial distribution of the gut microbiota are well-recognized as key pathogenic factors in the development of colitis.[58–60] Specifically, these alterations involve a decrease in beneficial bacterial populations, an increase in harmful bacteria, and changes in downstream metabolites mediated by the gut microbiota, all of which can exacerbate intestinal inflammation. In our study, we observed that DMY did not result in significant improvements in physiological parameters or intestinal barrier function in pseudo-germ-free colitis mice (Figures 7 and 8). Furthermore, it was noteworthy that the inhibitory effect of DMY on the expression of NLRP3 inflammasome proteins in the colon tissues of colitis mice was also abolished following the depletion of gut microbiota (Figure 8E). These findings strongly indicated that the gut microbiota acted as a critical mediator through which DMY alleviated colitis symptoms by inhibiting the NLRP3 inflammasome.

Conclusion

This study demonstrated that DMY effectively alleviated DSS-induced colitis in mice, as evidenced by partial restoration of the intestinal mucosal barrier, remodeling of dysbiotic gut microbiota, and modulation of aberrant immune responses. Specifically, DMY played a critical role in inhibiting inflammatory signaling and partially improving barrier function. Although the overall impact on colitis was limited, these effects contributed to improvements in intestinal health. Importantly, the potential molecular mechanism underlying DMY's anti-colitis effects involved its modulation of the gut microbiota, leading to inhibition of NLRP3 inflammasome activation. While DMY showed potential therapeutic value, further research is needed to fully elucidate its mechanisms and evaluate its clinical applicability.

Abbreviations

Abx, Antibiotic mixture; Cox-2, Cyclooxygenase-2; Cxcl1, C-X-C motif chemokine ligand 1; Cxcl10, C-X-C motif chemokine ligand 10; DAI, Disease activity index; DMY, Dihydromyricetin; DSS, Dextran sulfate sodium; H&E, Hematoxylin and eosin; Il-1β, Interleukin-1β; Il-6, Interleukin-6; INOS, Inducible nitric oxide synthase; LYM, Lymphocytes; MON, Monocytes; MPO, Myeloperoxidase; Nlrp3, NOD-like receptor pyrin domain containing 3; RT-qPCR, Quantitative real-time PCR; Tnf-α, Tumor necrosis factor-α; WBC, White blood cells.

Acknowledgments

This work was supported by joint supported by Special Scientific Research Projects for Double First-Class Construction of Hubei University of Chinese Medicine (NO. 2023ZZXJB001), Special Project of Hubei Provincial Technology Innovation Plan (NO. 2023BCB033), and Key Discipline Construction Project of Traditional Chinese Medicine in Hubei Province ([2023] No.2, Febrile Diseases).

Author Contributions

All authors made a significant contribution to the work reported, whether that is in the conception, study design, execution, acquisition of data, analysis and interpretation, or in all these areas; took part in drafting, revising or critically reviewing the article; gave final approval of the version to be published; have agreed on the journal to which the article has been submitted; and agree to be accountable for all aspects of the work.

Disclosure

The authors declare that they have no known competing financial interests or personal relationships that could have appeared to influence the work reported in this paper.

References

1. Ordas I, Eckmann L, Talamini M, Baumgart DC, Sandborn WJ. Ulcerative colitis. *Lancet*. 2012;380(9853):1606–1619. doi:10.1016/S0140-6736(12)60150-0
2. Zhao H, Wang Q, Zhao J, et al. Ento-A alleviates DSS-induced experimental colitis in mice by remolding intestinal microbiota to regulate SCFAs metabolism and the Th17 signaling pathway. *Biomed Pharmacother*. 2024;170:115985. doi:10.1016/j.biopha.2023.115985
3. Hu J, Mei Y, Zhang H, et al. Ameliorative effect of an acidic polysaccharide from Phellinus linteus on ulcerative colitis in a DSS-induced mouse model. *Int J Biol Macromol*. 2024;265(Pt 1):130959. doi:10.1016/j.ijbiomac.2024.130959
4. Le Berre C, Honap S, Peyrin-Biroulet L. Ulcerative colitis. *Lancet*. 2023;402(10401):571–584. doi:10.1016/S0140-6736(23)00966-2
5. Ng SC, Shi HY, Hamidi N, et al. Worldwide incidence and prevalence of inflammatory bowel disease in the 21st century: a systematic review of population-based studies. *Lancet*. 2017;390(10114):2769–2778. doi:10.1016/S0140-6736(17)32448-0
6. Feuerstein JD, Cheifetz AS. Ulcerative colitis: epidemiology, diagnosis, and management. *Mayo Clin Proc*. 2014;89(11):1553–1563. doi:10.1016/j.mayocp.2014.07.002
7. Hu Y, He Z, Zhang J, et al. Effect of Piper nigrum essential oil in dextran sulfate sodium (DSS)-induced colitis and its potential mechanisms. *Phytomedicine*. 2023;119:155024. doi:10.1016/j.phymed.2023.155024
8. Maloy KJ, Powrie F. Intestinal homeostasis and its breakdown in inflammatory bowel disease. *Nature*. 2011;474(7351):298–306. doi:10.1038/nature10208
9. Hao W, Cha R, Wang M, Zhang P, Jiang X. Impact of nanomaterials on the intestinal mucosal barrier and its application in treating intestinal diseases. *Nanoscale Horiz*. 2021;7(1):6–30. doi:10.1039/D1NH00315A
10. Groschwitz KR, Hogan SP. Intestinal barrier function: molecular regulation and disease pathogenesis. *J Allergy Clin Immunol*. 2009;124(1):3–20; quiz21–2. doi:10.1016/j.jaci.2009.05.038

11. Xu Q, Yao Y, Liu Y, Zhang J, Mao L. The mechanism of traditional medicine in alleviating ulcerative colitis: regulating intestinal barrier function. *Front Pharmacol*. 2023;14:1228969. doi:10.3389/fphar.2023.1228969
12. Eisenstein M. Gut reaction. *Nature*. 2018;563(7730):S34–s35. doi:10.1038/d41586-018-07277-1
13. Samoila I, Dinescu S, Costache M. Interplay between cellular and molecular mechanisms underlying inflammatory bowel diseases Development-A focus on ulcerative colitis. *Cells*. 2020;9(7):1647. doi:10.3390/cells9071647
14. Dharmasiri S, Garrido-Martin EM, Harris RJ, et al. Human intestinal macrophages are involved in the pathology of both ulcerative colitis and Crohn disease. *Inflamm Bowel Dis*. 2021;27(10):1641–1652. doi:10.1093/ibd/izab029
15. Mahmoud TN, El-Maadawy WH, Kandil ZA, et al. Canna x generalis L.H. Bailey rhizome extract ameliorates dextran sulfate sodium-induced colitis via modulating intestinal mucosal dysfunction, oxidative stress, inflammation, and TLR4/ NF-κB and NLRP3 inflammasome pathways. *J Ethnopharmacol*. 2021;269:113670. doi:10.1016/j.jep.2020.113670
16. Wang C, Liu Z, Zhou T, et al. Gut microbiota-derived butyric acid regulates calcific aortic valve disease pathogenesis by modulating GAPDH lactylation and butyrylation. *Imeta*. 2025;4(4):e70048. doi:10.1002/imt2.70048
17. Zhang R, Zhang H, Shi H, et al. Strategic developments in the drug delivery of natural product dihydromyricetin: applications, prospects, and challenges. *Drug Deliv*. 2022;29(1):3052–3070. doi:10.1080/10717544.2022.2125601
18. Zhang Q, Zhao Y, Zhang M, et al. Recent advances in research on vine tea, a potential and functional herbal tea with dihydromyricetin and myricetin as major bioactive compounds. *J Pharm Anal*. 2021;11(5):555–563. doi:10.1016/j.jpha.2020.10.002
19. Wang Y, Wang J, Xiang H, et al. Recent update on application of dihydromyricetin in metabolic related diseases. *Biomed Pharmacother*. 2022;148:112771. doi:10.1016/j.biopha.2022.112771
20. Liu D, Mao Y, Ding L, Zeng XA. Dihydromyricetin: a review on identification and quantification methods, biological activities, chemical stability, metabolism and approaches to enhance its bioavailability. *Trends Food Sci Technol*. 2019;91:586–597. doi:10.1016/j.tifs.2019.07.038
21. Wu J, Xiao Z, Li H, et al. Present status, challenges, and prospects of dihydromyricetin in the battle against cancer. *Cancers*. 2022;14(14):3487. doi:10.3390/cancers14143487
22. Zhang J, Chen Y, Luo H, et al. Recent update on the pharmacological effects and mechanisms of dihydromyricetin. *Front Pharmacol*. 2018;9:1204. doi:10.3389/fphar.2018.01204
23. Matouk AI, Awad EM, El-Tahawy NFG, El-Sheikh AAK, Waz S. Dihydromyricetin alleviates methotrexate-induced hepatotoxicity via suppressing the TLR4/NF-κB pathway and NLRP3 inflammasome/caspase 1 axis. *Biomed Pharmacother*. 2022;155:113752. doi:10.1016/j.biopha.2022.113752
24. Chu J, Wang X, Bi H, et al. Dihydromyricetin relieves rheumatoid arthritis symptoms and suppresses expression of pro-inflammatory cytokines via the activation of Nrf2 pathway in rheumatoid arthritis model. *Int Immunopharmacol*. 2018;59:174–180. doi:10.1016/j.intimp.2018.04.001
25. Dong S, Zhu M, Wang K, et al. Dihydromyricetin improves DSS-induced colitis in mice via modulation of fecal-bacteria-related bile acid metabolism. *Pharmacol Res*. 2021;171:105767. doi:10.1016/j.phrs.2021.105767
26. Wei X, Wu H, Wang Z, et al. Rumen-protected lysine supplementation improved amino acid balance, nitrogen utilization and altered hindgut microbiota of dairy cows. *Anim Nutr*. 2023;15:320–331. doi:10.1016/j.aninu.2023.08.001
27. Chen Y, Cui W, Li X, Yang H. Interaction between commensal bacteria, immune response and the intestinal barrier in inflammatory bowel disease. *Front Immunol*. 2021;12:761981. doi:10.3389/fimmu.2021.761981
28. Shi N, Li N, Duan X, Niu H. Interaction between the gut microbiome and mucosal immune system. *Mil Med Res*. 2017;4:14. doi:10.1186/s40779-017-0122-9
29. Moreira Lopes TC, Mosser DM, Goncalves R. Macrophage polarization in intestinal inflammation and gut homeostasis. *Inflamm Res*. 2020;69(12):1163–1172. doi:10.1007/s00011-020-01398-y
30. Xu Q, Sun W, Zhang J, et al. Inflammasome-targeting natural compounds in inflammatory bowel disease: mechanisms and therapeutic potential. *Front Immunol*. 2022;13:963291. doi:10.3389/fimmu.2022.963291
31. Khan N, Mukhtar H. Tea polyphenols in promotion of human health. *Nutrients*. 2018;11(1):39. doi:10.3390/nu11010039
32. Chen M, Zheng J, Zou X, et al. Ligustrum robustum (Roxb.) blume extract modulates gut microbiota and prevents metabolic syndrome in high-fat diet-fed mice. *J Ethnopharmacol*. 2021;268:113695. doi:10.1016/j.jep.2020.113695
33. Zhou X, Song Y, Zeng C, et al. Molecular mechanism underlying the regulatory effect of vine tea on metabolic syndrome by targeting redox balance and gut microbiota. *Front Nutr*. 2022;9:802015. doi:10.3389/fnut.2022.802015
34. Yang R, Wang Y, Mehmood S, et al. Polysaccharides from Armillariella tabescens mycelia mitigate DSS-induced ulcerative colitis via modulating intestinal microbiota in mice. *Int J Biol Macromol*. 2023;245:125538. doi:10.1016/j.ijbiomac.2023.125538
35. Qu L, Liu C, Ke C, et al. Atractylodes lancea rhizoma attenuates DSS-Induced colitis by regulating intestinal flora and metabolites. *Am J Chin Med*. 2022;50(2):525–552. doi:10.1142/S0192415X22500203
36. Tatiya-Aphiradee N, Chatuphonprasert W, Jarukamjorn K. Immune response and inflammatory pathway of ulcerative colitis. *J Basic Clin Physiol Pharmacol*. 2018;30(1):1–10. doi:10.1515/jbcpp-2018-0036
37. Jeon YD, Lee JH, Lee YM, Kim DK. Puerarin inhibits inflammation and oxidative stress in dextran sulfate sodium-induced colitis mice model. *Biomed Pharmacother*. 2020;124:109847. doi:10.1016/j.biopha.2020.109847
38. Hao W, Chen Z, Wang L, et al. Classical prescription Huanglian decoction relieves ulcerative colitis via maintaining intestinal barrier integrity and modulating gut microbiota. *Phytomedicine*. 2022;107:154468. doi:10.1016/j.phymed.2022.154468
39. Rohr MW, Narasimhulu CA, Rudeski-Rohr TA, Parthasarathy S. Negative effects of a high-fat diet on intestinal permeability: a review. *Adv Nutr*. 2020;11(1):77–91. doi:10.1093/advances/nmz061
40. Zong Y, Meng J, Mao T, et al. Repairing the intestinal mucosal barrier of traditional Chinese medicine for ulcerative colitis: a review. *Front Pharmacol*. 2023;14:1273407. doi:10.3389/fphar.2023.1273407
41. Wu S, Fang X, Zhao J, Liu G, Liao P. Nutrient regulation targeting macrophage-controlled intestinal mucosal healing: a promising strategy against intestinal mucositis induced by deoxynivalenol. *Toxicon*. 2025;264:108434. doi:10.1016/j.toxicon.2025.108434
42. Schroeder BO. Fight them or feed them: how the intestinal mucus layer manages the gut microbiota. *Gastroenterol Rep*. 2019;7(1):3–12. doi:10.1093/gastro/goy052
43. Wan L, Qian C, Yang C, et al. Ginseng polysaccharides ameliorate ulcerative colitis via regulating gut microbiota and tryptophan metabolism. *Int J Biol Macromol*. 2024;265(Pt 2):130822. doi:10.1016/j.ijbiomac.2024.130822

44. Luo Y, Fu S, Liu Y, et al. Banxia Xiexin decoction modulates gut microbiota and gut microbiota metabolism to alleviate DSS-induced ulcerative colitis. *J Ethnopharmacol*. 2024;326:117990. doi:10.1016/j.jep.2024.117990
45. Ghosh S, Whitley CS, Haribabu B, Jala VR. Regulation of intestinal barrier function by microbial metabolites. *Cell Mol Gastroenterol Hepatol*. 2021;11(5):1463–1482. doi:10.1016/j.jcmgh.2021.02.007
46. Zafar H, Saier MH. Gut bacteroides species in health and disease. *Gut Microbes*. 2021;13(1):1–20. doi:10.1080/19490976.2020.1848158
47. Li S, Han X, Liu N, et al. Lactobacillus plantarum attenuates glucocorticoid-induced osteoporosis by altering the composition of rat gut microbiota and serum metabolic profile. *Front Immunol*. 2023;14:1285442. doi:10.3389/fimmu.2023.1285442
48. Cheng J, Liu D, Huang Y, et al. Phlorizin mitigates dextran sulfate sodium-induced colitis in mice by modulating gut microbiota and inhibiting ferroptosis. *J Agric Food Chem*. 2023;71(43):16043–16056. doi:10.1021/acs.jafc.3c01497
49. Li L, Li T, Liang X, et al. A decrease in Flavonifractor plautii and its product, phytosphingosine, predisposes individuals with phlegm-dampness constitution to metabolic disorders. *Cell Discov*. 2025;11(1):25. doi:10.1038/s41421-025-00789-x
50. Guo H, Callaway JB, Ting JP. Inflammasomes: mechanism of action, role in disease, and therapeutics. *Nat Med*. 2015;21(7):677–687. doi:10.1038/nm.3893
51. Gong Z, Zhao S, Zhou J, et al. Curcumin alleviates DSS-induced colitis via inhibiting NLRP3 inflammsome activation and IL-1β production. *Mol Immunol*. 2018;104:11–19. doi:10.1016/j.molimm.2018.09.004
52. Shao BZ, Xu ZQ, Han BZ, Su DF, Liu C. NLRP3 inflammasome and its inhibitors: a review. *Front Pharmacol*. 2015;6:262. doi:10.3389/fphar.2015.00262
53. Coll RC, Schroder K, Pelegrin P. NLRP3 and pyroptosis blockers for treating inflammatory diseases. *Trends Pharmacol Sci*. 2022;43(8):653–668. doi:10.1016/j.tips.2022.04.003
54. Pandey SN, Babu MA, Goyal K, et al. Targeting NLRP3 inflammasome with curcumin: mechanisms and therapeutic promise in chronic inflammation. *Inflammopharmacology*. 2025;33(10):5667–5687. doi:10.1007/s10787-025-01926-4
55. Guo X, Xu Y, Geng R, Qiu J, He X. Curcumin alleviates dextran sulfate sodium-induced colitis in mice through regulating gut microbiota. *Mol Nutr Food Res*. 2022;66(8):e2100943. doi:10.1002/mnfr.202100943
56. Yu B, Wang Y, Tan Z, et al. Resveratrol ameliorates DSS-induced ulcerative colitis by acting on mouse gut microbiota. *Inflammopharmacology*. 2024;32(3):2023–2033. doi:10.1007/s10787-024-01456-5
57. Hu E, Li Z, Li T, et al. A novel microbial and hepatic biotransformation-integrated network pharmacology strategy explores the therapeutic mechanisms of bioactive herbal products in neurological diseases: the effects of Astragaloside IV on intracerebral hemorrhage as an example. *Chin Med*. 2023;18(1):40. doi:10.1186/s13020-023-00745-5
58. Guo XY, Liu XJ, Hao JY. Gut microbiota in ulcerative colitis: insights on pathogenesis and treatment. *J Dig Dis*. 2020;21(3):147–159. doi:10.1111/1751-2980.12849
59. Ren DD, Chen KC, Li SS, et al. Panax quinquefolius polysaccharides ameliorate ulcerative colitis in mice induced by dextran sulfate sodium. *Front Immunol*. 2023;14:1161625. doi:10.3389/fimmu.2023.1161625
60. Zhang XJ, Yuan ZW, Qu C, et al. Palmatine ameliorated murine colitis by suppressing tryptophan metabolism and regulating gut microbiota. *Pharmacol Res*. 2018;137:34–46. doi:10.1016/j.phrs.2018.09.010